Control of single-phase islanded PV/battery streetlight cluster based on power-line signaling

Quintana, Pablo; Garcia, Jorge; Guerrero, Josep M.; Dragicevic, Tomislav; Vasquez, Juan Carlos

Published in:
Proceedings of the 2013 International Conference on New Concepts in Smart Cities: Fostering Public and Private Alliances (SmartMILE)

DOI (link to publication from Publisher):
10.1109/SmartMILE.2013.6708213

Publication date:
2013

Document Version
Early version, also known as pre-print

Control of single-phase islanded PV/battery streetlight cluster based on Power-Line Signaling

Pablo J. Quintana†, Jorge Garcia†, Josep M. Guerrero*, Tomislav Dragicevic* and Juan C. Vasquez*
†CE3I2 Research Group. Department of Electrical and Electronics Engineering. University of Oviedo, SPAIN
*Microgrids Research Group. Department of Energy Technology. Aalborg University, DENMARK
Email: quintanapablo@uniovi.es, garciajorge@uniovi.es, joz@et.aau.dk, tdr@et.aau.dk, juq@et.aau.dk

***Abstract*—Power regulation of all converter units in a microgrid should not be only determined by load demand, but also by the available power of each unit, i.e. a converter fed by a battery. Energy management control is essential in order to handle the variety of prime movers which may include different types of renewable energy sources (RES) and energy storage systems (ESS). Specifically, the recharging process of secondary battery, the most prominent ESS, should be done in a specific manner to preserve its life-time, microgrid line voltage must be kept within the bounds and the energy offered by RES should be utilized as efficiently as possible. This paper proposes a coordinated control strategy based on power-line signaling (PLS), instead of common communications, for a single-phase minigrid in which each unit can operate in different operation modes taking into account the resource limitation. The whole system is explained ahead and finally, simulation results obtained in Simulink are presented to validate the proposed control strategy.**

On the other hand, the proposed loads are several electromagnetic ballast driving high pressure sodium (HPS) lamps. Although this kind of ballast are not installed nowadays, this paper is proposed for a recent installation where is not worth to change these devices due to lack of amortization.

Index Terms- Single-phase, minigrid, microgrid, PLS, electromagnetic, ballast

I. Introduction

CLASSICAL power systems make use of large power plants located far from the consumption points, at adequate places and transferring all the generated power through long, expensive transmission lines. This power system has to be continuously regulated by control centers to ensure the quality of the power, voltage and frequency. Nevertheless, nowadays this way of procedure is changing slowly but uninterruptedly due to the increasing number of dispersed distributed generation units (DG) and the integration of distributed storage systems (DS), including both renewable and non-renewable sources, like ESS [1]. The installation of small wind turbines and photovoltaic (PV) generators at user's home has become a new trend in many countries, so, in order to deal with them and also with the dispersed loads, intelligent microgrids appear to be a good solution. This will be a key point to cope with new functionalities, as well as to integrate RES into the grid. Those small grids should be able to generate and store energy near to the consumption points. This avoids large distribution lines coming from big power plants located far away from the consumption areas [2]. DG units are usually low cost, low voltage and low power (typically microturbines, PV and batteries). Power electronics provide the control and flexibility required by a microgrid [3], [4].

978-1-4799-2911-5/13/$31.00 ©2013 IEEE

A microgrid can be operated either in island mode or grid-connected with similar configuration [5]. The main difference remains in the power balance in islanded microgrids, where energy generation and power consumption must be in equilibrium and well coordinated [6]. Due to the intermittent nature of RES, added together with unpredictable load fluctuations, may cause instantaneous power unbalances that affect the operation of the microgrid. Hence, ESS are required to guarantee reliability, security and power stability [7]. A common mode of working is using RES to provide the maximum power they can to the loads and the ESS as a backup compensator, absorbing and injecting power when it is possible and/or necessary. If the batteries of the ESS are completely charged, the absorption of extra power from RES is not allowed, so they have to reduce the injection of power and work in another equilibrium point, lower than the maximum [2]. However, a practical islanded system may suffer from the lack of power generation or energy storage. These possible situations requires to work in a flexible way combining maximum power point tracker (MMPT) algorithms for RES with the state of charge (SoC) of the ESS. A good coordination between RES and ESS can make the difference between a reliable microgrid and a non-stable one.

For the coordination of RES and ESS in ac stand-alone sytems, many techniques have been proposed. Some of them make use of central supervisory controllers with communication setups [8], [9]. However, since the control capability could be the best, the reliability is not suitable for a such sensitive and complex system. Moreover, with an increase in the number of units, their connectivity may require extensive hardware [7], [10].

In [11], a concept named distributed bus signaling (DBS) is proposed to avoid the use of a central controller for communications. This class of control methods are commonly used for industrial islanded systems in order to send messages to other points of the grid without the special need of a physical emitter and a demodulator. However, even though the need for supervisory controller is eliminated when DBS strategy is used, some other major issues are opened: for instance, fixed common voltage deviations are inherent to particular system operating mode, limiting the number of modes that can be reliably used [7]. In order to deal with this disadvantages, in

[12] a method based on PLS is proposed for a three phase ac power system. The concept consists of using the power lines as carriers of sinusoidal logic signals only and the PLS has been proposed as a more flexible extension of DBS. The advantage over DBS is that instead of having fixed voltage deviation throughout the particular operating mode, PLS signals are used as triggers for mode transitions where deviation can be optionally canceled by secondary control action without affecting proper operation [7]. Moreover, for typical small-scale stand-alone power systems, the use of this method is quite recommended, but it is not for big grids with resistive lines due to the fact that the signal can be lost during the process.

This paper presents an islanded single-phase minigrid formed by one ESS which will be the master inverter that will generate the nominal voltage and frequency of 230 V rms and 50 Hz, and two RES. These RES consist of two independent groups of PV panels, that means both units are totally independent in terms of power generation. As the minigrid fulfill the previous premise of being a small-scale system, the use of a PLS is a good proposal in order to coordinate all the converters and control quite accurately the charge of the battery.

The paper is organized as follows. Section II is dedicated to explain the model use to simulate the loads. In Section III is presented the physical configuration of the minigrid and the primary control of each of the elements is revised: it will be explained how the decisions are taken in function of the SoC of the battery. Section IV is dedicated to show the proposed PLS distributed energy management strategy, how the PLS frequency was chosen and also how to isolate this signal from the main voltage at 50 Hz, which is much bigger. In Section V are presented many issues related to the control of all the converters: inner loops, calculation of frequencies and angles for synchronous transformations, SoC estimation algorithm or the MPPT method. Straightaway, some simulation results obtained with the dSPACE will be shown in Section VI. Finally, it will be reached the part of Conclusions and Future developments.

II. Lighting systems based on electromagnetic ballasts. Model

The model of the conventional low frequency electromagnetic ballast and the 150W HPS lamp was taken from real devices and built in Simulink. This model is needed to simulate the line current demanded by the real loads, which are conventional LF electromagnetic streetlamps. From the real ballast and lamp, real data were taken, which are summarize in Table I:

TABLE I: Parameters of the minigrid

Parameter	Value
Ballast current	1 A
Ballast voltage	320 V
Lamp current	2.7 A
Lamp voltage	108 V
Ballast resistance	5.5 Ω
Ballast inductance	325 mH
Ballast capacitance	20 μF

In [13], [14] different techniques and models for HPS lamps are presented. The behavior of these models is accurate but generally complex to develop.

In this paper, a simpler model was done in order to be easy to simulate. However, despite its simplicity, the information given about the harmonics generation in the grid is reliable and its behavior is precise in comparison with the real values. The lamp model is based on the voltage-source behavior of the lamp discharge at low frequency. Two zener diodes in anti-series configuration model the basic behavior of the discharge, being the zener voltage the arc voltage of the lamp, with a value of 95V. Two exponential curves, used to model the time constants of the re-ignition peak have also been added to this basic model. As a result, the final lamp model is presented in Fig. 1. In Fig. 2 is shown the data obtained from the real model and the characteristic curve I vs. V of the lamp.

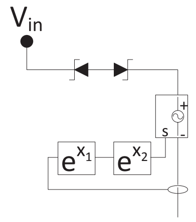

Fig. 1: Model of the lamp.

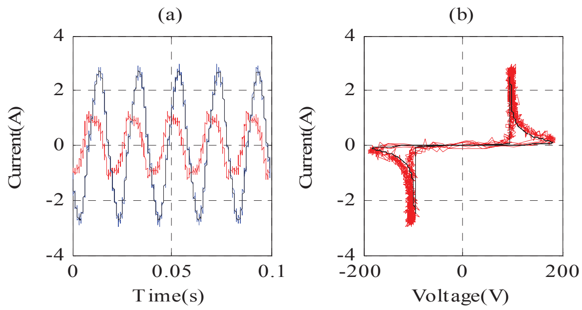

Fig. 2: (a) Red: real measured ballast current; blue: real measured lamp current; black: simulated lamp current. (b) I vs. V curve characteristic of the lamp.

III. Minigrid structure

In Fig. 3 is shown an islanded single-phase minigrid which is made by a ESS unit and two RES ones. In this configuration, ESS will work as a voltage source and RES, as they collaborate injecting power, will operate as current mode voltage sources inverters (CM-VSI). As it was explained in Section I, in general, in order to take the more possible advantage from renewables, RES units operate at the maximum power point. However, renewable power is usually kind of unpredictable, so a backup power is needed. Thus, the batteries have to be always available to compensate the likely variations in the power given by RES or demanded by the loads. Since in some cases, the power at the MPPT supplied by RES is bigger than the needed by the loads and hence there is a battery system, the best option is to charge the energy storage devices while it is possible. The SoC will increase while this injection of current continues, but when it reaches certain value, this extra power must be reduced in order to protect the batteries and avoid the destruction of the device. Hence, a coordinated control of RES based on the SoC of the batteries is needed and it can be basically stated in three points:

- SoC is below 95%: keep RES at MPPT.
- SoC reaches 95%: begin to smoothly move the operating point of the PV panels, reducing in this way the power injected in the minigrid.
- At some moment, ESS needs to supply a load and SoC starts to decrease. PV panels begin to go back to the MPP.

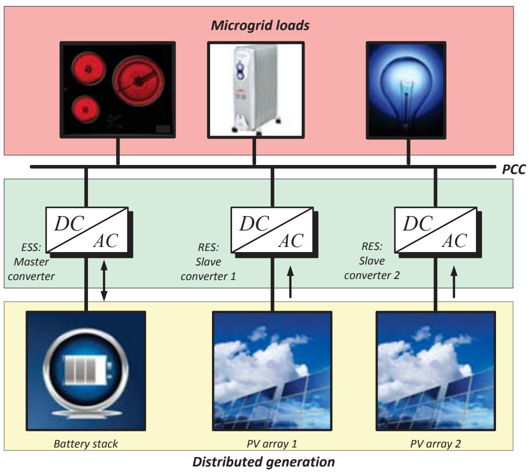

Fig. 3: Diagram of a small-scale minigrid.

IV. PLS PRINCIPLE AND PROPOSED CONTROL TECHNIQUE

In order to control RES units without communications, in this paper is used a technique previously done in [12] but adapted to a single-phase minigrid needs. For decades, the power utilities have employed frequency droop to realize real power sharing among the generation facilities. Considering one facility, as power draw increases, the frequency is decreased. This reduces the phase angle of the voltage from that plant relative to the rest of the network [12]. Each plant has a droop coefficient associated with its output rating such that all the plants lower their frequency. Eventually, all the plants will have the same frequency and each will be putting out the same per-unit power. As the total load on the network increases, the frequency will decrease. The frequency of the network, therefore, indicates the per unit load on the system [12].

In the proposed technique, a small ac voltage signal is injected into the system as a control signal. When RES units detect it, they will start to decrease the injected power. When the SoC reaches the minimum level to activate the PLS, it will be injected by the master converter. Hence, this small signal will not be always in the minigrid, but only when it is necessary to control RES units. In order to detect this signal, the procedure will be:

- measure the capacitor voltage at the capacitor of the RES filter,
- filter the voltage and extract the desired frequency,
- use a phase-locked loop (PLL) to detect the value of this frequency,
- depending on this value, calculate the new operating point of the PV panel.

A. *Selection of the PLS frequency*

In order to avoid any kind of conflict with key frequencies, like the harmonic ones for a 50 Hz grid, the selection of the signal's frequency has to be done wisely. In [12] is given a clue, taking into account possible sidebands around the selected frequency affected by the fundamental. In this paper, the selected frequency range has been 175-180 Hz. Thus, there is no objection with harmonics or any other consideration. In Fig. 4 it can be seen the distribution of the harmonic content and how the PLS does not have any special relevance. Typical loads can be roughly divided into passive and active ones, but all of them are usually designed for a specific main range of frequencies (50 to 60 Hz). The introduction of a small signal of 170 Hz does not affect its behavior.

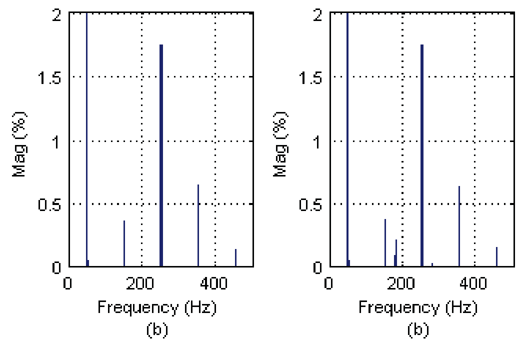

Fig. 4: Frequency analysis: (a) Before injecting PLS (b) After injecting PLS.

B. *Detection of the PLS*

As it can be seen in Fig. 4, this signal is very small in comparison with the line voltage, so high order filters are needed [12]. In this paper, a fourth-order bandpass filter was tuned in series with a bandstop, in order to reduce to the minimum the 50 Hz component, which is much bigger (see Fig. 5).

After having the signal filtered, a PLL is able to detect the frequency and give a precise value.

C. *Control of the PV panels with the PLS*

As it was said, the injection of the PLS is used to control the power that the PV panels are giving to the minigrid. When the PLL detects it, the MPPT algorithm freezes and does not try to keep looking for the maximum power. In addition, an increment in the voltage reference for the PV panel related to the frequency of the PLS is added to the previous MPPT voltage, reducing this way the current supplied by the RES.

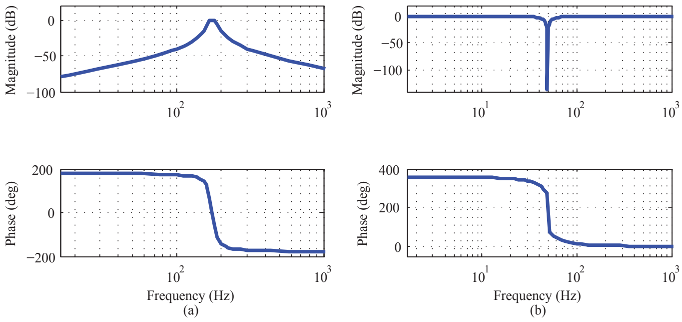

Fig. 5: Bode diagram: (a) Bandpass (b) Bandstop.

Thus, the way of controlling the power the PV panels inject in the minigrid is by slightly modifying the operating point. In Fig. 6 is shown how the frequency of the injected signal to make the communications varies in function of the SoC of the battery. Until a 95%, the PLS is not injected, which means that the frequency is zero, but, nevertheless, beyond this SoC, this frequency begins to increase until a certain value, in this case, 180 Hz.

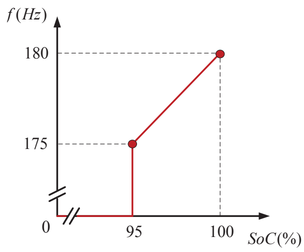

Fig. 6: PLS frequency selection depending on the SoC.

V. Control strategy implementation

In Fig. 7 is shown a summary control scheme that represents the whole system. ESS unit (the master converter) is controlled by two inner loops, as shown in Fig. 7: a voltage and a current loop. This inner loops are aiming at achieving good output capacitor voltage regulation. All the control was done in a synchronous reference frame (dq), hence, for this master inverter, the transformation from a single-phase signal to a dq one is done by calculating the synchronous angle in function of the frequency and then using Park transformation.

On the other hand, both RES units work as CM-VSI. This means that there are only one inner loop, a current one, which assures the injection of the current precisely in the minigrid. Nevertheless, in this case, the transformation to a synchronous reference frame can not be achieved by using the same method as with the master inverter due to the lack of data transmission between all the stations. The way to do it is by means of a SOGI-PLL [15]. Measuring the voltage, a SOGI-PLL is able to track the frequency of the signal (and basically, the phase angle), thus doing the transformation to dq is now possible.

Because of the use of the synchronous reference frame, all the signals are not sinusoidal anymore, so PI regulators were used to control all the variables. They are described as (1):

$$G_{in}(s) = k_p + \frac{k_i}{s} \tag{1}$$

A. SoC estimation

The SoC is estimated by ampere-hour (Ah) counting method expressed in (2).

$$SoC = SoC(0) - \int_0^t \frac{I_{bat}(t)}{C_{bat}} dt \tag{2}$$

where SoC(0) represents the initial SoC, C_{bat} is the capacity of the battery and I_{bat} is the current of the battery [16].

B. MPPT algorithm

The selected method in this paper for tracking the maximum power point of the PV panels was the classical Hill-climbing algorithm. There are many different and better options ([17], [18], [19]) to track this point and since it is out of the scope of this work, the easiest way to do it was chosen. On the other hand, despite of this fact, this model is able to find the operating point with changes in the temperature of the PV panel and oscillations in the irradiation due to possible shadows or other circumstances.

Fig. 8 shows a basic flowchart where it is described the main decisions taken by the control algorithm.

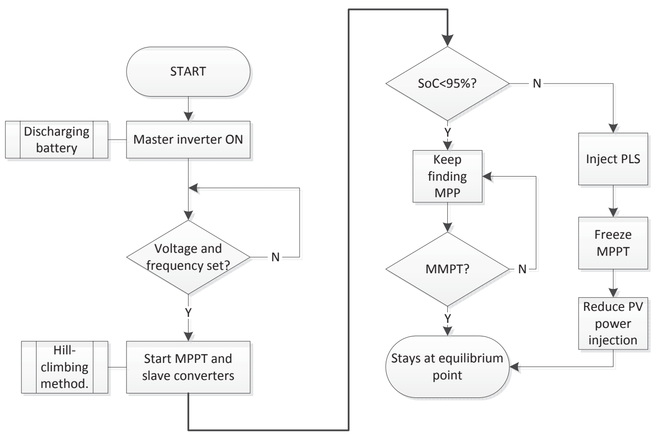

Fig. 8: General flowchart for the whole system.

VI. Simulation results

First of all, Table II summarizes the main parameters of the system.

Fig. 9 shows the results which have been obtained and all the transitions will be detailed next. Initially, just the ESS is feeding the load, thus, the SoC of the battery decreases. In $t = 10s$, both RES units are started up and they begin to find the maximum operating point. It can be seen that in Fig. 9b or in Fig. 9c how they increase continuously their power and at the same time how the power the battery is giving is reduced, even below 0, the point where it changes to charging mode, at approximately $t = 20s$ (Fig. 9f).

It can be seen that this process goes on without changes until $t = 42s$, when battery reaches 95% of the SoC and the power

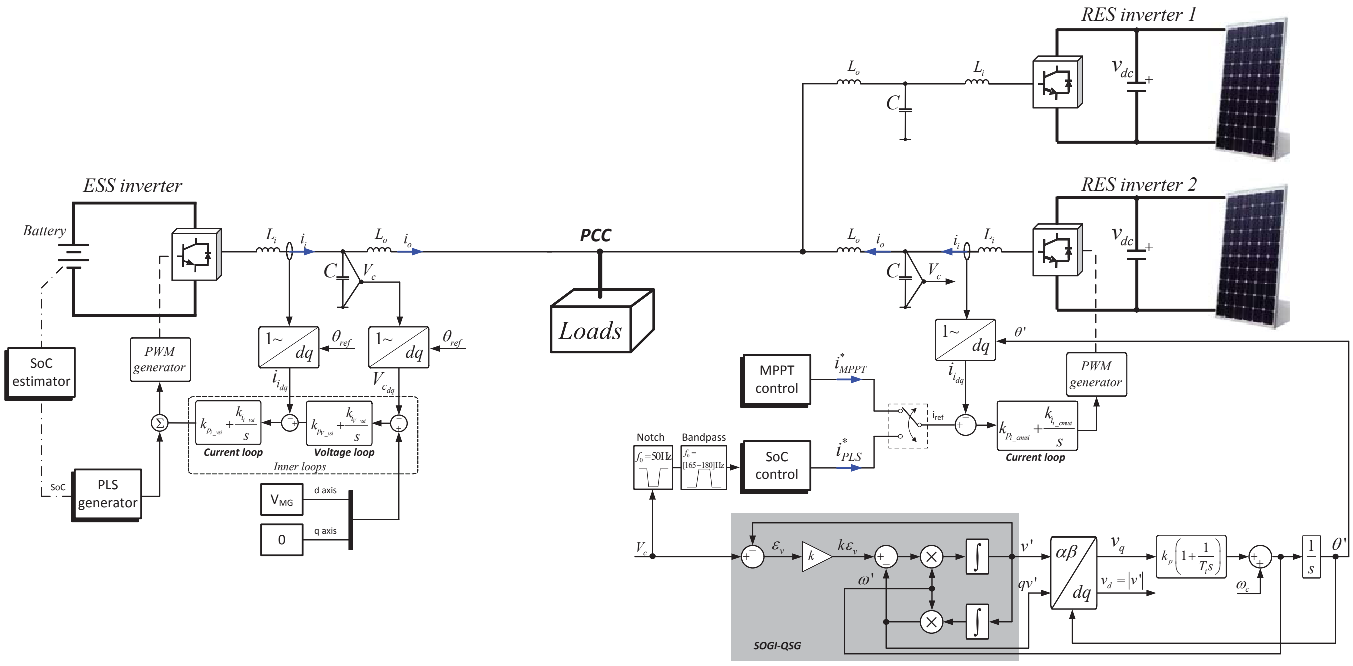

Fig. 7: Control scheme of the minigrid.

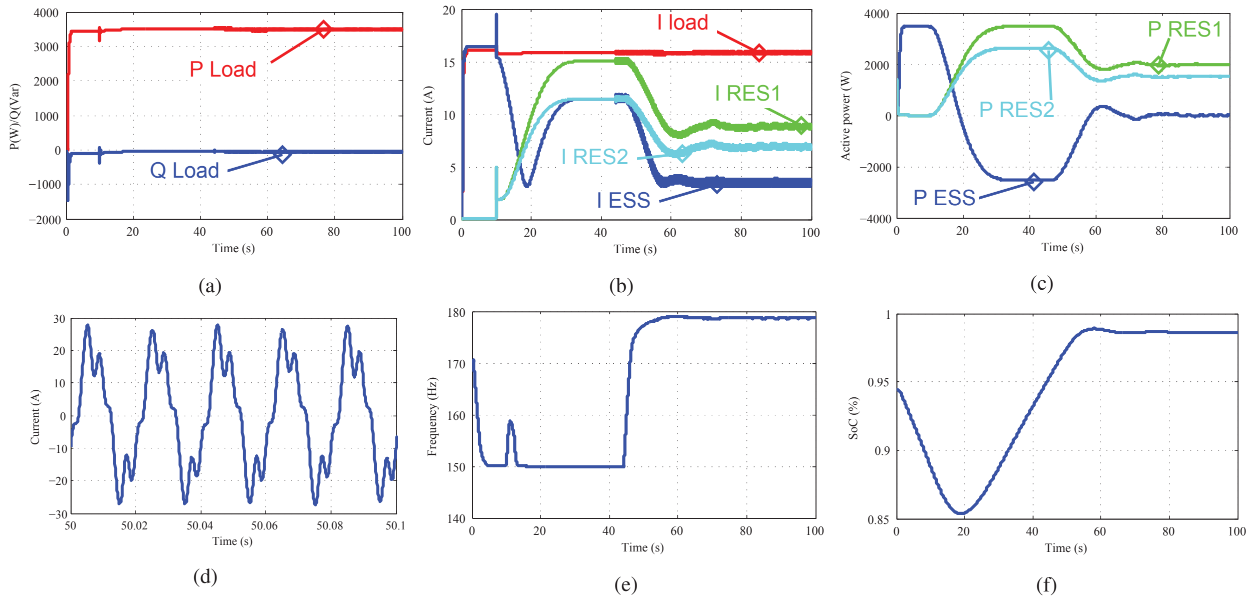

Fig. 9: Simulation results: (a) Load active and reactive power (b) RMS currents (c) Active power of the converters (d) Current demanded by the loads (e) PLS frequency detected with the PLL (f) SoC of the battery.

given by RES units starts to get reduced until a new operation point is found. This operating point is the one where the load is feed just with renewable energies and ESS unit waits as a backup. In Fig. 9e can be seen the frequency that the PLL is giving. When there is no PLS injection, PLL stays at a certain frequency.

VII. Conclusion

In this paper has been presented a coordinated control strategy for islanded single-phase minigrids based on PLS communications. The aim is to coordinate ESS and RES unit to deal with the situation of source limitation. This PLS has been used in order to coordinate all the units without any communication link or a wireless one. Then, it has been shown the simulation results obtained with Simulink and how all the units work together to find an operating point that minimizes the power given by the battery. Having a look to the results, it has sense to say that the expandability of proposed method to more units is possible, always taking into account that a PLS is possible for small-scale stand-alone power systems but it is not for big grids with resistive lines due to the fact that the signal can be lost during the process.

TABLE II: Parameters of the minigrid

Parameter	Symbol	Value
Nominal output voltage	V_{ref}	230 V
Nominal output frequency	f_{ref}	50 Hz
Filter input inductor	L_i	1.8 mH
Filter output inductor	L_o	1.8 mH
Filter capacitor	C	27 μF
Current integral Term (ESS)	$k_{pI_{vsi}}$	10
Current integral Term (RES)	$k_{pI_{cmvsi}}$	40
Voltage integral Term (ESS)	$k_{pV_{vsi}}$	2
Current proportional Term (ESS)	$k_{pI_{vsi}}$	1.8
Current proportional Term (RES)	$k_{pV_{cmvsi}}$	15
Voltage proportional Term (ESS)	$k_{pV_{vsi}}$	0.2

VIII. Future developments

Although in this paper, the voltage and the frequency references are given directly to the master converter, there is another possibility that is using a droop control for this unit. If this droop control is activated, a secondary control can be implemented to restore the voltage and the frequency to the nominal values. This issue was done and will be implemented and improved in future works.

Another improvement will be to help ESS unit with reactive power, if it would be necessary, with RES units. By doing this, the battery could remain completely charged during more time through the day and all its capacity would be used at night.

Finally, install more than one ESS unit would be an important issue, but, nevertheless, synchronization between two or more master inverters needs a different strategy and a very precise control in order to keep a good power sharing.

Acknowledgment

This work was supported by the Spanish Government, Innovation and Science Office (MICINN), under research grant no. DPI-2010-15889, project ”Enerlight”, by the European Union through the ERFD structural funds (fondos FEDER) and by Aalborg University, where the authors did the work. The authors would also like to thank all the people who belong to the Microgrid Group of Aalborg University their help and support.

References

[1] S. Heier, *Grid Integration of Wind Energy Conversion Systems*. 2006.

[2] J. Vasquez, J. Guerrero, J. Miret, M. Castilla, and L. de Vicu “Hierarchical control of intelligent microgrids,” *Industrial Electronics Magazine, IEEE*, vol. 4, no. 4, pp. 23–29, 2010.

[3] R. Lasseter, “Microgrids,” in *Power Engineering Society Winter Meeting, 2002. IEEE*, vol. 1, pp. 305–308 vol.1, 2002.

[4] P. Piagi and R. Lasseter, “Autonomous control of microgrids,” in *Power Engineering Society General Meeting, 2006. IEEE*, pp. 8 pp.–, 2006.

[5] F. Blaabjerg, R. Teodorescu, M. Liserre, and A. Timbus, “Overview of control and grid synchronization for distributed power generation systems,” *Industrial Electronics, IEEE Transactions on*, vol. 53, no. 5, pp. 1398–1409, 2006.

[6] F. Katiraei, M. Iravani, and P. Lehn, “Micro-grid autonomous operation during and subsequent to islanding process,” *Power Delivery, IEEE Transactions on*, vol. 20, no. 1, pp. 248–257, 2005.

[7] T. Dragicevic, J. Guerrero, J. Vasquez, and D. Skrlec, “Supervisory control of an adaptive-droop regulated dc microgrid with battery management capability,” *Power Electronics, IEEE Transactions on*, vol. 29, no. 2, pp. 695–706, 2014.

[8] D. Olivares, C. Canizares, and M. Kazerani, “A centralized optimal energy management system for microgrids,” in *Power and Energy Society General Meeting, 2011 IEEE*, pp. 1–6, 2011.

[9] J.-Y. Kim, S.-K. Kim, and J.-H. Jeon, “Coordinated state-of-charge control strategy for microgrid during islanded operation,” in *Power Electronics for Distributed Generation Systems (PEDG), 2012 3rd IEEE International Symposium on*, pp. 133–139, 2012.

[10] Q. Shafiee, J. Vasquez, and J. Guerrero, “Distributed secondary control for islanded microgrids - a networked control systems approach,” in *IECON 2012 - 38th Annual Conference on IEEE Industrial Electronics Society*, pp. 5637–5642, 2012.

[11] K. Sun, L. Zhang, Y. Xing, and J. Guerrero, “A distributed control strategy based on dc bus signaling for modular photovoltaic generation systems with battery energy storage,” *Power Electronics, IEEE Transactions on*, vol. 26, no. 10, pp. 3032–3045, 2011.

[12] A. Tuladhar, H. Jin, T. Unger, and K. Mauch, “Control of parallel inverters in distributed ac power systems with consideration of line impedance effect,” *Industry Applications, IEEE Transactions on*, vol. 36, no. 1, pp. 131–138, 2000.

[13] W. Wei, Z. Guo-dong, and X. Dian-guo, “A physics-based model for hid lamps with rectifying effect,” in *Vehicle Power and Propulsion Conference, 2008. VPPC ’08. IEEE*, pp. 1–5, 2008.

[14] W.-L. Chen and Y.-Y. Hsu, “Direct output voltage control of a static synchronous compensator using current sensorless d-q vector-based power balancing scheme,” in *Transmission and Distribution Conference and Exposition, 2003 IEEE PES*, vol. 2, pp. 545–549 vol.2, 2003.

[15] M. Ciobotaru, R. Teodorescu, and F. Blaabjerg, “A new single-phase pll structure based on second order generalized integrator,” in *Power Electronics Specialists Conference, 2006. PESC ’06. 37th IEEE*, pp. 1–6, 2006.

[16] “Ieee guide for optimizing the performance and life of lead-acid batteries in remote hybrid power systems,” 2008.

[17] T. Noguchi, S. Togashi, and R. Nakamoto, “Short-current pulse-based maximum-power-point tracking method for multiple photovoltaic-and-converter module system,” *Industrial Electronics, IEEE Transactions on*, vol. 49, no. 1, pp. 217–223, 2002.

[18] D. Sera, R. Teodorescu, J. Hantschel, and M. Knoll, “Optimized maximum power point tracker for fast-changing environmental conditions,” *Industrial Electronics, IEEE Transactions on*, vol. 55, no. 7, pp. 2629–2637, 2008.

[19] N. Femia, G. Petrone, G. Spagnuolo, and M. Vitelli, “Optimization of perturb and observe maximum power point tracking method,” *Power Electronics, IEEE Transactions on*, vol. 20, no. 4, pp. 963–973, 2005.